

Cite this: *RSC Pharm.*, 2026, **3**, 126

# An evaluation of the pharmaceutical properties of the Nigerian baobab polysaccharide for sustained release oral tablets

Munirah A. Ajiboye,<sup>a</sup> Yogesh Rawat,<sup>b</sup> Nihad Mawla,<sup>a</sup> Rand Abdulhussain,<sup>a</sup> Haja Muhamad,<sup>a</sup> Adeola O. Adebisi,<sup>a</sup> Barbara R. Conway,<sup>a</sup> Alan M. Smith,<sup>a</sup> Gordon A. Morris,<sup>b</sup> Katie Addinall,<sup>b</sup> Maria Dimopoulou,<sup>c</sup> Athanasios Angelis-Dimakis<sup>b</sup> and Kofi Asare-Addo<sup>b</sup>                                                                                                                                                                                                                                                                                                                                                                                                            

referred to as “Kuka”. Due to the various traditional uses of the baobab tree in medicine and nutrition, it is commonly referred to as the “chemist tree”.<sup>11,12</sup> Polysaccharides extracted from the baobab tree generally contain high molecular weight random coiled chains with particularly high intrinsic viscosity depending on the extraction process.<sup>13</sup> Depending on the technology or solvent employed for the extraction process, different polysaccharides with distinct physicochemical compositions, macromolecular and structural characteristics, and functional and biological characteristics can be achieved.<sup>12,14</sup> Polysaccharides extracted from the baobab fruit pulp have been shown to contain linear xylogalacturonans<sup>8,13</sup> with small amounts of co-extracted glucans<sup>15</sup> depending on the pH used for extraction.<sup>8</sup> Polysaccharides extracted from baobab, as with polysaccharides extracted from other novel sources, are referred to as pectin-like polysaccharides as they usually consist of lower amounts of galacturonic content (<65%) and larger amounts of neutral sugars (glucose, arabinose, rhamnose and galactose) and therefore cannot be classified as pectin for pharmaceutical or food applications.<sup>16</sup> Pectin is a complex polysaccharide present in the wall of plant cells. Pectin has been investigated as an excipient in a variety of dosage forms, including film coatings for colon-specific drug delivery systems with ethyl cellulose, microparticulate delivery systems for ophthalmic preparations, and matrix-type transdermal patches. Although it has great potential as a hydrophilic polymeric material for controlled release matrix drug delivery systems, its water solubility adds to the drug's premature and rapid release from these matrices.<sup>1,17</sup> Pectin can form gels in a variety of ways depending on its structure. Gelation can be induced by acidification, cross-linking with calcium ions, or the alginate reaction.<sup>2</sup> Research shows that it has a molecular composition (phenolic compounds, galacturonic acid, acetyl groups, proteins and neutral sugars) that makes it suitable for use in pharmaceutical applications.<sup>10,13,18,19</sup>

This study first aimed at extracting baobab polysaccharide from the oblong fruit and characterising its solid-state properties. An investigation into the mechanical properties of the Nigerian baobab polysaccharide relevant to its use as an excipient was conducted. The study then sought to investigate the polysaccharide as a potential matrix former to control the release of a model drug (theophylline) in a bid to encourage the use of abundant renewable sources of raw materials suitable for use in the pharmaceutical industry in the developing world.

## 2. Materials and methods

### 2.1. Materials

The oblong-shaped baobab (*Adansonia digitata*) fruit was dried at 45 °C and ground to a fine powder before being subjected to extraction. For the extraction process, all buffer salts, sodium azide, disodium phosphate heptahydrate, monosodium phosphate monohydrate, ethanol and dialysis membranes (molecular weight cut-off 12 000 Da) were purchased from Sigma

Aldrich (Gillingham, UK) and were of analytical grade. Microcrystalline cellulose (MCC) (Avicel PH101) was purchased from FMC (Pentre, UK), magnesium stearate was purchased from Merck (Darmstadt, Germany) and theophylline, the model drug used, was purchased from TCI Chemicals (Oxford, UK). pH 6.8 buffer solutions used for dissolution analysis consisting of sodium hydroxide and potassium phosphate monobasic were purchased from Fisher Scientific (Loughborough, UK) and Honeywell Fluka (Loughborough, UK), respectively. The pH 1.2 medium was prepared using hydrochloric acid purchased from Fisher Scientific (UK) and potassium chloride was purchased from Honeywell Fluka (Loughborough, UK).

### 2.2. Extraction of the baobab polysaccharide

718.6 g of the dried Nigerian baobab fruit sample was used in the extraction process. The polysaccharide was extracted on a bench scale according to the experimental design that was reported in ref. 20 and 21 with minor modifications. The first step was aqueous extraction (pH 6.0) at 80 °C for 1 h at a mass ratio of 1 : 25. Subsequently, the extracted material was cooled and neutralised (pH 7) with sodium hydroxide at 25 °C, followed by centrifugation, rotary evaporation at 80 °C, ethanol precipitation and overnight storage. The precipitate was centrifuged, oven-dried at 60 °C for 1 h and finally extensively dialysed against distilled water (molecular weight cut-off: 12 000 Da) and oven dried at 60 °C for 48 h. This whole process is depicted in Fig. 1.

The obtained polysaccharide from the extraction process was milled with a Retsch ball mill (Retsch MM400). A frequency of 30 Hz for 2 min was used to reduce the particle size of the produced extract and the final powder was passed through a 250 µm sieve, which was sealed and stored till required.

### 2.3. Solid-state characterisation of the baobab polysaccharide

**2.3.1. Differential scanning calorimetry (DSC).** The method reported in ref. 22 was adopted without modification. The Mettler Toledo DSC1 instrument was used for DSC experimentation under a nitrogen atmosphere with approximately 2.5 mg of the Nigerian baobab polysaccharide powder weighed into a standard aluminium crucible and crimped. The heating rate was 10 °C min<sup>-1</sup> from 25 °C to 600 °C.

**2.3.2. Thermogravimetric analysis (TGA).** TGA was carried out using the Mettler Toledo DSC1 instrument. The baobab polymer (~20 mg) was directly weighed into 70 µl alumina pans under a nitrogen atmosphere at a flow rate of 50 cm<sup>3</sup> min<sup>-1</sup>. The heating rate was 10 °C min<sup>-1</sup> from 25 °C to 600 °C.

**2.3.3. X-ray powder diffraction (XRPD).** In brief, the powder was scanned in Bragg–Brentano geometry, from 5° to 100° in 0.02° steps at 1.5° min<sup>-1</sup> using a D2 Phaser diffractometer (Bruker AXS GmbH, Karlsruhe, Germany). A sealed microfocus generator operated at 30 kV in 10 mA scan mode, producing CuKα ( $\lambda = 0.1542$  nm) radiation, and equipped with a Lynxeye silicon strip multi-angle detector was used, as reported in ref. 22.



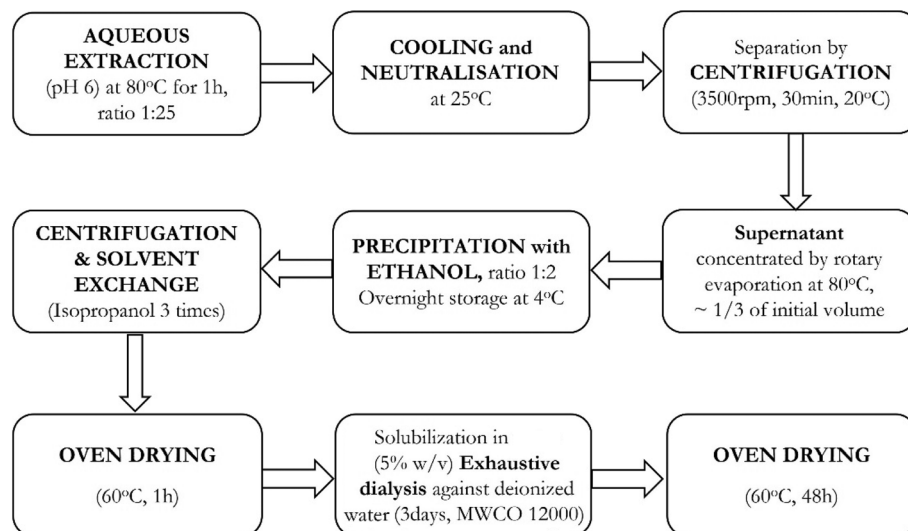


Fig. 1 Extraction protocol of the baobab polysaccharide from the baobab oblong-shaped fruit.

**2.3.4. Keyence imaging/measurement.** Acquisition of grain images was performed using focus-stacking digital microscopy (Keyence VHX-7000). Images were captured at  $\times 300$  magnification using HDR (High Dynamic Range) and full-ring lighting with an exposure time of 10 ms. The focus plane was adjusted manually to ensure that the  $z$  (vertical) axis envelope encompasses all points of focus within the sample. Using vertical imaging steps of 100  $\mu\text{m}$ , 13 separate images were acquired of the sample, which were then combined into one image stack, where all the surface depths were in focus. Width measurements were then acquired using inbuilt measurement software, specifically employing the manual two-point measurement function.

#### 2.4. Preparation of tablets and mechanical strength

A Tubular™ mixer (Willy A. Bachofen, Switzerland) was used to mix the Nigerian baobab polysaccharide powder, microcrystalline cellulose, theophylline and magnesium stearate as per the ratios in Table 1. Each batch was prepared using 5 g of powder mixture, which included all excipients and the active pharmaceutical ingredient. All the components shown in Table 1 without the magnesium stearate were mixed for 8 min to ensure uniformity, after which magnesium stearate was then added and then the final blend was mixed for a further 2 min.

**2.4.1. True density, bulk density, tapped density and Carr's index.** The true densities of the pure Nigerian baobab polysaccharide powder and the powder blends (Table 1) were measured using a gas pycnometer – Micrometrics Accupyc II 1340 (Micrometrics, USA). Approximately 1 gram of powder was used for each true density measurement using a helium pycnometer. The true density of the sample was acquired in triplicate. The bulk density of the Nigerian baobab polysaccharide was determined by carefully pouring a pre-weighed portion of the powder into a measuring cylinder and recording the volume (bulk volume). The measuring cylinder was then tapped until there was no change in volume (tapped volume). The measurements of the tapped and bulk volumes and pre-determined powder weight were used to calculate the bulk and tapped densities. Tablet porosity was also calculated using the true and bulk densities measured (as in eqn (1)) to determine its effect on the varying baobab polysaccharide concentrations on the tablet matrices:

$$\text{Porosity \%} = \left( 1 - \frac{\text{True density}}{\text{Bulk density}} \right) \times 100 \quad (1)$$

**2.4.2. Tablet compaction of baobab polysaccharide and formulations.** Using a Testometric machine (M500-50 CT) and a 10 mm flat die, 200 mg of the pure baobab polysaccharide was compacted at five different forces (5 kN, 7.5 kN, 10 kN, 12.5 kN, and 15 kN) producing flat-faced circular tablets. The formulations, as tabulated in Table 1, were compacted at 10 kN to

Table 1 Batch formula for preparation of powder blends of the baobab polysaccharide

Formulation code	Baobab polysaccharide (%)	Theophylline (%)	MCC (%)	Magnesium stearate (%)
B1	10	41.5	47.5	1
B2	20	41.5	37.5	1
B3	30	41.5	27.5	1
B4	50	41.5	7.5	1
B5	57.5	41.5	0.0	1



produce  $300 \pm 1$  mg tablets. The tablet thickness and diameter were measured immediately after compression and after a recovery time of 24 h using a digital caliper (Mitutoyo Kawasaki, Japan). Three tablets from each of the produced compacts were fractured to determine their mechanical strength using a hardness tester (Pharma Test hardness device, Germany). 20 tablets were made from each formulation batch.

## 2.5. Tablet swelling

The swelling behaviour of the baobab polysaccharide tablets was investigated using a digital camera (Leica ICC50HD) linked to Keyence image analysis software. A tablet compact was placed vertically in a plastic Petri dish, and 70 mL of deionized water was added at ambient temperature. The Petri dish was placed on a plane with a light source (tungsten lamp), and the camera, equipped with a macro lens, was placed above. The data were obtained at 20 min intervals for up to 120 min. The swelling index study was performed in triplicate.

## 2.6. *In vitro* dissolution testing

The *in vitro* theophylline release was carried out using an automated USP Type II (paddle method) dissolution apparatus, Pharma Test DT 70 (PharmaTest, Germany). Dissolution vessels were filled with 900 mL of dissolution media (acid solution (pH 1.2) or buffer solution (pH 6.8)) equilibrated to a temperature of  $37 \pm 0.5$  °C with a paddle speed of 50 rpm. Dissolution was studied from 10 min to 240 min, with the theophylline content in the samples primed automatically at a set time point by a pump into an attached UV spectrophotometer, where the theophylline content was measured with the UV spectrophotometer at 286 nm. All experiments were conducted in triplicate.

**2.6.1. Dissolution parameters.** Eqn (2) was used to calculate the mean dissolution time (MDT), which is the amount of time needed for a drug to dissolve under the current dissolving conditions and is appropriate for dosage forms with various drug release mechanisms.<sup>7,23,24</sup> The area under the curve up to a specific time  $t$ , which is stated as a percentage area of a rectangle by 100% dissolution in the same period  $t$ , is what is referred to as the dissolution efficiency (DE). DE was calculated using eqn (3) (ref. 7 and 24), where  $j$  is the sample number,  $n$  is the number of dissolution samples,  $t_j$  is the time at the midpoint between  $t_j$  and  $t_{j-1}$ ,  $\Delta M_j$  is the additional amount of drug dissolved between  $t_j$  and  $t_{j-1}$ , and  $y$  represents the drug percentage dissolved at time  $t$ .

$$\text{MDT} = \frac{\sum_{j=1}^n t_j \Delta M_j}{\sum_{j=1}^n \Delta M_j} \quad (2)$$

$$\text{DE} = \frac{\int_0^t y \times dt}{y_{100} \times t} \times 100 \quad (3)$$

**2.6.2. Similarity factor.** The similarity between the drug release profiles was determined using the similarity factor  $f_2$  according to eqn (4):

$$f_2 = 50 \times \log \left\{ \left[ 1 + \frac{1}{n} \sum_{t=1}^n (R_t - T_t)^2 \right]^{-0.5} \times 100 \right\} \quad (4)$$

This is a mathematical treatment of the dissolution data, where  $n$  = number of pull points for tested samples;  $R_t$  = reference assay at time point  $t$ ; and  $T_t$  = test assay at time point  $t$ .

The similarity factor was calculated using the drug release profile obtained from the formulation containing 57.5% baobab polysaccharide content (B5) as the reference standard. An  $f_2$  value ranging from 50 to 100 suggests a similarity in the test and the reference drug release profiles.<sup>7</sup> The closer the  $f_2$  value is to 100, the more similar or identical the release profiles are. Additionally, dissimilarity occurs with a decrease in the  $f_2$  value.<sup>25</sup>

**2.6.3. Kinetics of drug release.** Drug release kinetics in solid oral dosage forms can be characterized using different models, each describing different mechanisms and rates of release. In this study, zero-order, first-order, Higuchi, and Korsmeyer–Peppas models were considered to investigate the release profiles of the tablets.

The zero-order model represents a constant rate of drug release, independent of the drug concentration,<sup>26,27</sup> as shown in the following equation:

$$Q = Q_0 + k_0 t \quad (5)$$

where  $Q$  is the cumulative amount of drug released over time  $t$ ,  $Q_0$  is the initial amount of drug (often zero), and  $k_0$  is the zero-order release constant.

In contrast, in the first-order kinetics, the drug release is directly proportional to the remaining drug concentration,<sup>28</sup> expressed as

$$\ln(Q_t) = \ln(Q_0) + k_1 t \quad (6)$$

where  $Q$  is the amount of drug released over time  $t$ ,  $Q_0$  is the initial drug quantity and  $k_1$  represents the first-order rate constant.

The Higuchi model describes drug release in systems where the concentration of the drug exceeds its solubility, leading to release rates that follow the square root of time.<sup>29</sup> This relationship is represented by

$$M_t = k_H \sqrt{t} \quad (7)$$

with  $M_t$  representing the cumulative amount of drug released at time  $t$  and  $k_H$  is the Higuchi release constant.

The Korsmeyer–Peppas (power-law model) is used for cases where drug release mechanisms may involve diffusion, swelling, or matrix dissolution. In this model:

$$\frac{M_t}{M_\infty} = k t^n \quad (8)$$

where  $M_t/M_\infty$  is the fraction of drug released at time  $t$ ,  $k$  is a constant related to the drug release that considers the matrix geometry, and  $n$  is the diffusional exponent of drug release. For cylinders, which were the shape of the tablet matrices made in this study,  $n$  values of up to 0.45 suggest Fickian diffusion, and values above 0.89 suggest Case-II transport. A



value between these two suggests anomalous transport as reported in numerous studies.<sup>30</sup>

### 3. Results and discussion

#### 3.1. Extraction and solid-state properties of the baobab polysaccharide

The extraction of polysaccharides from baobab fruit involved several steps, as shown in Fig. 1. The process resulted in 144 g (20% yield) of polysaccharide extract from the dried sample. Our bench-scale yield for Nigerian oblong baobab (20%) is lower than literature values for similar protocols (~29–30% from oblong/oval fruits), but techno-economic analysis indicates viability when ethanol is recycled and utilities are optimised. Published models report minimum selling prices of ~£23–£35 per 100 g in the UK at ~30% yield and ~£27 per 100 g in Nigeria, with steam cost being the dominant sensitivity.<sup>31</sup> Using focus stacking digital microscopy, the maximum grain width of the extracted, milled and sieved polysaccharide was found to be 115  $\mu\text{m}$  (Fig. 2a). The XRPD data for the extracted baobab polysaccharide suggest that it is completely amorphous in nature (Fig. 2b) with broad halos,<sup>32,33</sup> which have also been observed in *Grewia* polysaccharides.<sup>30</sup>

Thermal stability is an essential characteristic that determines the processing conditions and potential uses of polysaccharides. TGA and DSC analyses were carried out over a range of temperatures between 25  $^{\circ}\text{C}$  and 600  $^{\circ}\text{C}$  as shown in Fig. 3a and b. During the TGA analysis, weight loss occurred in three phases, which is a typical behaviour for polysaccharide decomposition.<sup>34</sup> The first weight loss of approximately 13.1% is seen to occur due to water loss.<sup>30,34</sup> When the temperature was increased to 175  $^{\circ}\text{C}$ , the TGA showed a major mass change of approximately 49%, which may be due to the deterioration of the polysaccharide structure at 250  $^{\circ}\text{C}$ .<sup>35,36</sup> The final stage of degradation occurred between 300  $^{\circ}\text{C}$  and 500  $^{\circ}\text{C}$  with approximately 11% weight loss. The last two phases coincided

with the broad endothermic enthalpy change in DSC, as seen in Fig. 3b. The char yield of the sample was 37%. The thermal analysis studies on the sample indicate that, after accounting for the initial water loss, the material is stable until around 175  $^{\circ}\text{C}$ , after which thermal degradation takes place.

#### 3.2. Physical properties of the baobab polysaccharide and formulation blends and tablets

The true density of the pure baobab (milled baobab polysaccharide from a <250  $\mu\text{m}$  sieve) was calculated to be 1.63  $\text{g cm}^{-3}$  with the bulk and tap densities recorded as  $0.73 \pm 0.01$  and  $0.97 \pm 0.01$   $\text{g cm}^{-3}$ , respectively, giving the baobab polysaccharide a Carr's consolidation index of 29%, which is indicative of poor flow properties.

The compaction profiles of the polysaccharide (milled baobab polysaccharide from a <250  $\mu\text{m}$  sieve) from 5 kN to 15 kN are depicted in Fig. 4. This shows the tablet porosity and mechanical strength of the compacted baobab polysaccharide properties. Fig. 4 shows that an increase in the compression and compaction of the polysaccharide led to an increase in the mechanical strength of the compacts, which was accompanied by a simultaneous decrease in the porosity of the compacts. This increase in mechanical strength with an increase in compression has been observed and reported for other polysaccharides.<sup>22</sup> This showed that the extracted polysaccharide is a compressible polysaccharide and therefore has the potential for use in tableted formulations.

Formulations B1–B5 (Table 1) had true densities similar to that of the pure baobab polysaccharide (1.55–1.59  $\text{g cm}^{-3}$ ). This slight decrease upon blending with other formulation components has also been observed and reported.<sup>30</sup> It is important to note that all formulation blends were compacted at 10 kN only. It was observed that there was a general increase in the tablet's mechanical strength with an increase in the MCC content in the formulation (68–148 kN) (Fig. 5). MCC has been reported to be used widely for direct compression to reduce tablet density and has good mechanical strength.<sup>37,38</sup>

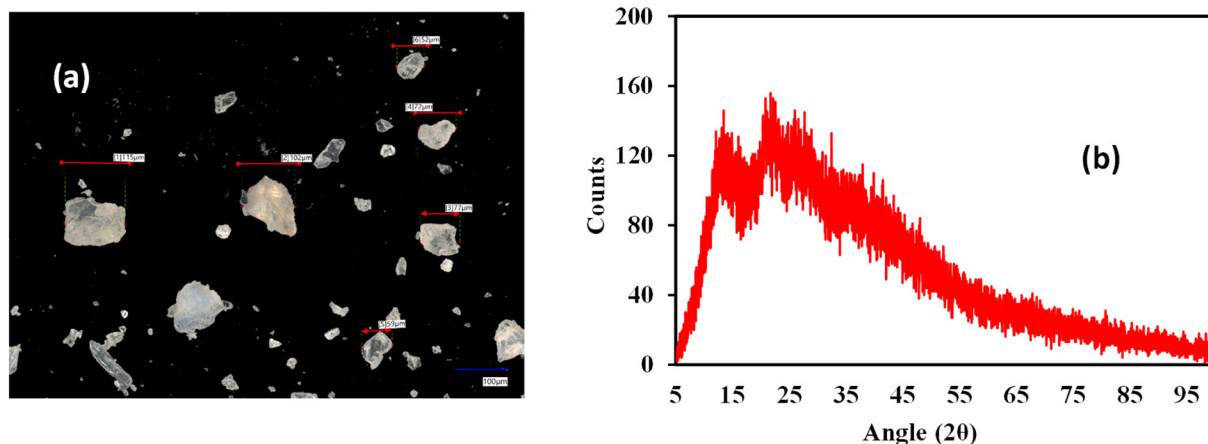


Fig. 2 Measurement of the grain width of the baobab polysaccharide with two-point measurement. (a) Original image of the grain sample  $\times 300$ . Scale bar is 100  $\mu\text{m}$ . (b) XRPD pattern of the extracted and milled baobab polysaccharide from a <250  $\mu\text{m}$  sieve.



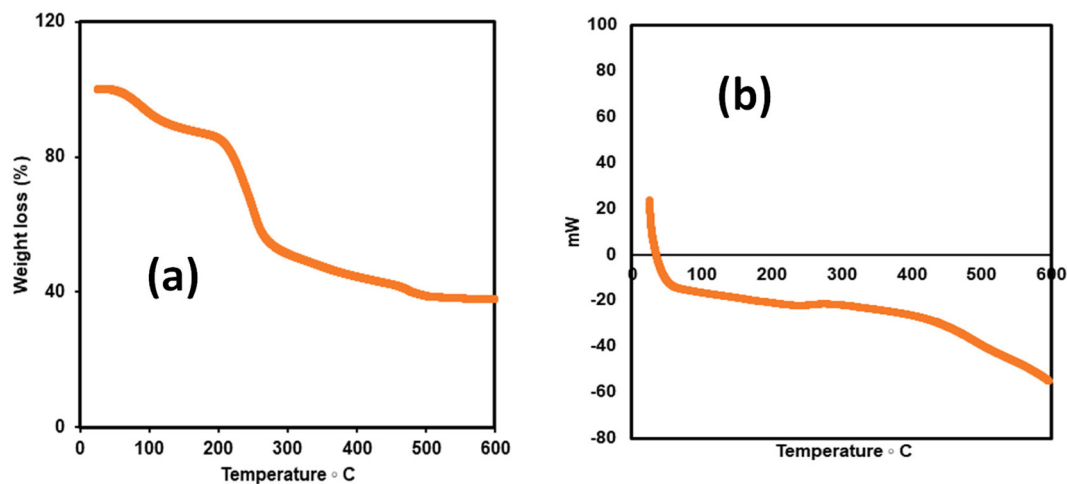


Fig. 3 (a) TGA and (b) DSC thermograms of the milled baobab polysaccharide from a <250  $\mu\text{m}$  sieve.

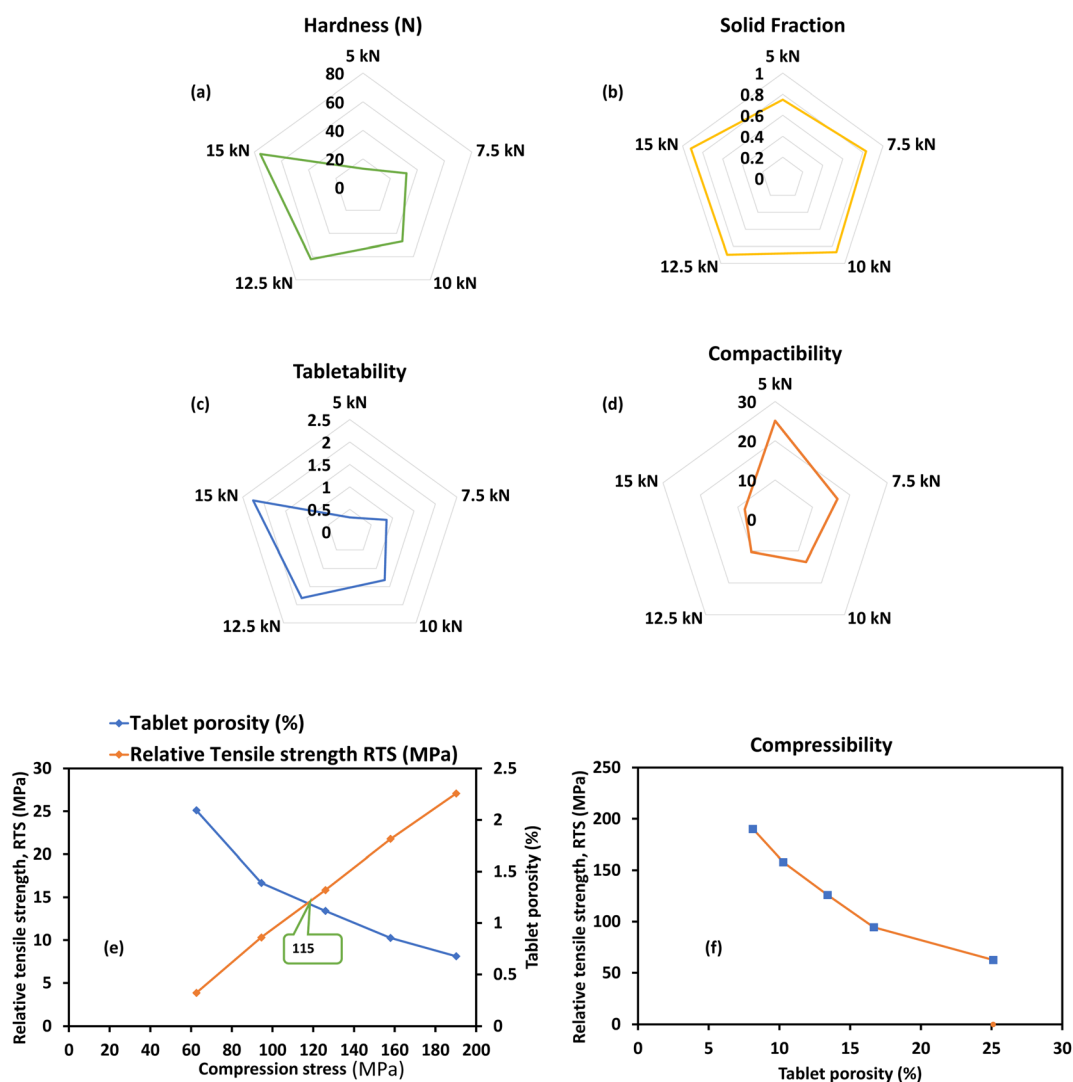


Fig. 4 Properties of compacted baobab polysaccharide (milled baobab polysaccharide from a <250  $\mu\text{m}$  sieve) under 5 kN–15 kN: (a) compact hardness, (b) solid fraction, (c) tableability, (d) compactibility, (e) compression stress relationship with tablet porosity and relative tensile strength and (f) tablet porosity relationship with tensile strength. All experiments were conducted in triplicate.



The porosities of the formulated blends ranged from 9–11% demonstrating a real impact of the formulation changes on the porosity of the compacts. This suggests that porosity may not necessarily be a contributing factor to potential dissolution performance.

### 3.3. Tablet swelling

The swelling capacity of tablets compacted with the pure baobab polysaccharide powder was evaluated in deionized water. The process was set for the compacts to be evaluated for up to 120 min; however, the swelling of the compacts lasted for 45 min only. The compacts at this time point were observed to have lost their structure and began to gradually dissolve in the Petri dish (Fig. 6). A similar behaviour for *Grewia* polysaccharides has been reported in deionised media. The authors however reported different behaviours for the *Grewia mollis* polysaccharide at pH 12 and pH 6.8.<sup>22</sup> Such observed behaviour can impact drug release. It has been reported in the literature that the composition of ions in a medium can impact drug release.<sup>7,22,25,30</sup>

### 3.4. Theophylline release from baobab polysaccharide tablets

Drug release in acidic media is shown in Fig. 7a. Fig. 7a illustrates how the acid solution used as the release medium influences theophylline release from the tablet matrices with five differing baobab concentrations. The solubility of theophylline is largely unchanged over the pH range studied. Theophylline's solubility at pH 1.2 has been reported to be  $13.1 \pm 0.1 \text{ mg ml}^{-1}$  and  $10.5 \pm 0.1 \text{ mg ml}^{-1}$  at pH 6.8.<sup>39</sup> There was a gradual release of theophylline from all the tablet matrices (B2–B5) except for those containing 10% baobab (B1), which showed a relatively faster release of theophylline. It is important to note that all tablets contain the same amounts of

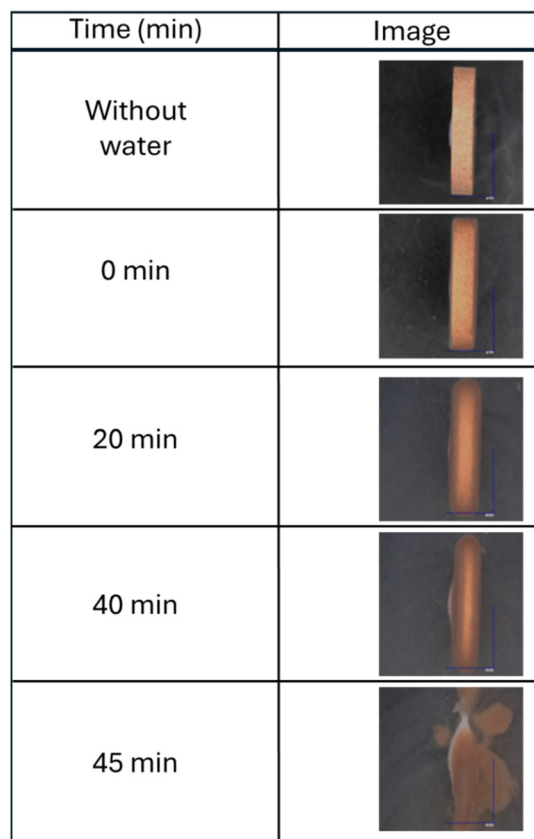


Fig. 6 Photograph of pure baobab polysaccharide tablets swelling in deionized water over a 45 min time period. All experiments were conducted in triplicate.

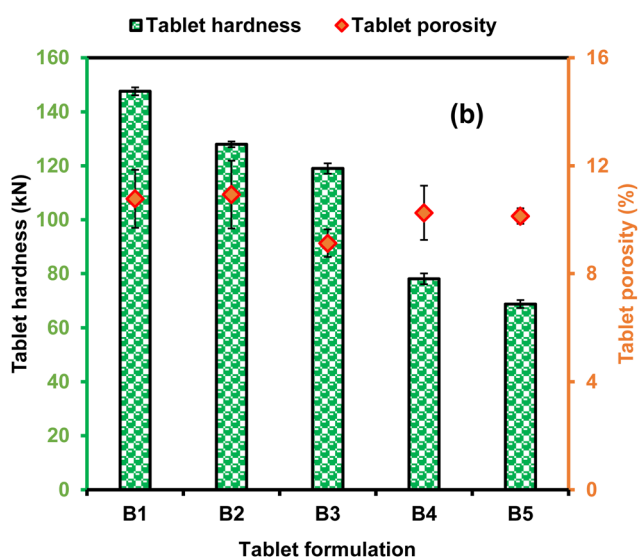


Fig. 5 Formulated tablet properties of hardness and porosity using the baobab polysaccharide. Note: formulations B1–B5 have constituents as identified in Table 1. All experiments were conducted in triplicate.

theophylline content (41.5%) and magnesium stearate (1%). After about 10 min in acidic media, the profiles of B2–B5 showed that 12.6% of theophylline was released from the tablets containing 20% baobab with 37.5% MCC (B2), 11.8% of theophylline was released from tablets containing 30% baobab with 27.5% MCC, 9.43% of theophylline was released from tablets containing 50% baobab and 9.9% from tablets containing 57.5% baobab with no MCC, indicating no burst release. This shows a gradual decrease in the initial release of the model drug with an increase in baobab content.

The drug release after 240 min for formulations B2–B5 are relatively similar (Fig. 7a). This is also confirmed in Table 2, where the dissolution parameters of DE (52–54%), MDT (78–92 min) and MDR ( $0.37\text{--}0.40\% \text{ min}^{-1}$ ) are similar. Using drug release from B5 (baobab-only matrices) as the reference standard,  $f_2$  values indicated similarity (71–77%). It was not possible to determine MDT and MDR for the B1 dissolution profile due to its quick release. Its profile was dissimilar to the reference standard (B5) used ( $f_2 = 18\%$ ). The faster release also made it impossible to determine its kinetics of drug release. When baobab was used alone with no further excipients, the matrices had an  $n$  value of 0.68, which suggests that anomalous transport occurred. This was also the case for formulations B2–B4. It was however interesting to note that there



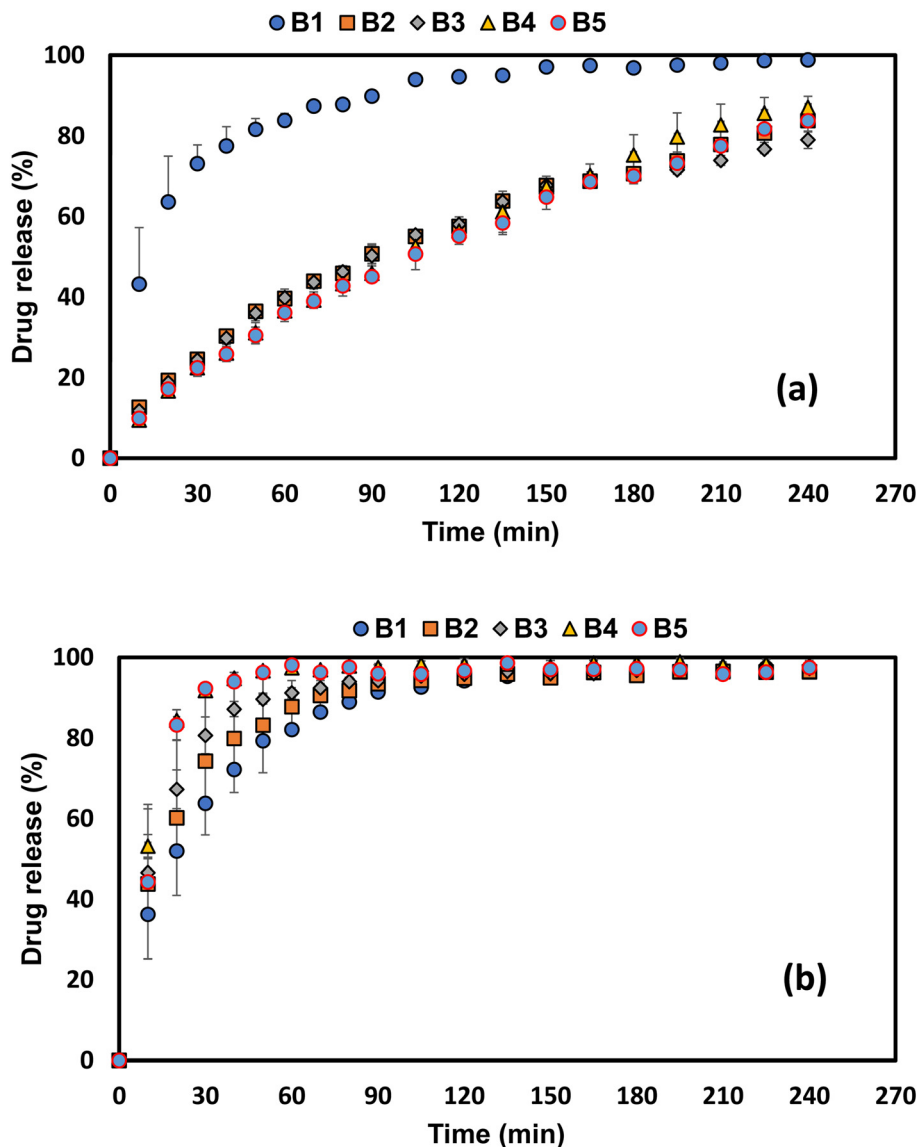


Fig. 7 Effect of theophylline release from baobab polysaccharide matrices in acidic media (a) and basic media (b). All experiments were conducted in triplicate. Note: formulation codes B1–B5 are explained in Table 1.

was an increase in the contribution of erosion with an increase in baobab content associated with a decrease in the MCC content. The incorporation of MCC therefore seems to be really advantageous for improving the tablet hardness of the manufactured matrices as well, indicating to a formulator that there may well be a concentration where it might be inadequate or not be beneficial as in the case of formulation B1.

In contrast to drug release in acidic media, in buffer, the tablets containing 10% baobab with 47.5% MCC (B1) released approximately 36.3% of theophylline in the first 10 min, 43.8% of theophylline was released from the 20% baobab with 37.5% MCC (B2), and 46.6% of theophylline was released from the 30% baobab with 27.5% MCC (B3). The tablets containing 50% baobab powder with 7.5% MCC (B4) released approxi-

mately 53.2% of theophylline. This showed that an increase in the baobab content contributed to the burst release observed in the phosphate buffer media. Of interest, however, was the behaviour of the baobab-only matrices (B5), *i.e.*, the tablets containing 57.5% baobab with no MCC content. These matrices released approximately 44% of theophylline after 10 min but released their total drug content relatively faster than all the matrices with MCC content. This suggests that MCC may have a beneficial effect in reducing burst release in phosphate buffer media. The faster release of theophylline (after 240 min, the tablet matrices were completely dissolved for all five formulations) meant that it was not possible to calculate dissolution parameters and kinetics for drug release in the buffer. The viscosity of baobab fruit polysaccharide has been studied in both acidic and basic media using a Kinexus



**Table 2** Dissolution parameters for baobab matrices released in acidic media

Formulation code	Powder formulation	MDT (min)	DE (%)	MDR (% min <sup>-1</sup> )	Similarity factor ( <i>f</i> <sub>2</sub> )	Zero order (RSQ)	First order (RSQ)	Higuchi (RSQ)	Peppas (RSQ)	Diffusion exponent ( <i>n</i> )
B1	10% BBP + 47.5% MCC + drug	—	15.88	—	17.94	—	—	—	—	—
B2	20% BPP + 37.5% MCC + drug	84.53	54.28	0.38	73.18	0.970	0.993	0.996	0.997	0.625
B3	30% BPP + 27.5% MCC + drug	77.78	53.41	0.37	71.26	0.972	0.995	0.998	0.997	0.653
B4	50% BPP + 7.5% MCC + drug	89.05	51.76	0.40	77.26	0.985	0.998	0.997	0.997	0.710
B5	57.5% BPP + drug	91.62	51.79	0.37	—	0.981	0.998	0.997	0.997	0.676

All experiments were conducted in triplicate.

rheometer (Malvern Instruments, UK) fitted with a 20 mm plate-plate geometry and a 1 mm gap.<sup>21</sup> The authors reported that an increase in temperature by applying the time-temperature superposition principle results in a monotonic reduction of both viscoelastic functions ( $G'$ ,  $G''$ ). The authors also found that although the shape of the curves produced remained unchanged (meaning no measurable structural changes), the construction of the master curves of viscoelasticity revealed significant differences in the relaxation behaviour of samples at different pH values. The samples in acidic media were found to be typical of entangled viscoelastic chains, indicating a strong frequency dependency.<sup>21</sup> This behaviour is thus attributed to the observed performance of the polysaccharides in different media. It is therefore anticipated that the baobab polysaccharide in combination with the MCC therefore forms a swelling gel matrix which hinders drug diffusion, slows down the drug release, and thus eliminates significant burst release. This behaviour has been observed in the literature for hydrophilic matrices as acidic media enhance hydrogen bonding and gel formation.<sup>40,41</sup> This suggests that the baobab polysaccharide might not be suitable for targeting drug release in the lower small intestine or colon. These dissolution behaviours also explain why porosity is not a likely dominant release-controlling factor.

## 4. Conclusion

The extraction process for the baobab polysaccharide was efficient and therefore feasible for large-scale production. The extracted polysaccharide however had poor flow properties, as indicated by its true density and Carr's index. When incorporated into tablet formulations as a potential matrix former, it is compressible and forms tablets or compacts with adequate mechanical strength. In acidic media, tablets with higher baobab content (formulations B2–B5) demonstrated a slower, more controlled release of theophylline. The absence of burst release in formulations with higher baobab content (B4 and B5) further supports

its potential for use in controlled release systems. In basic media, tablets with higher baobab content (B4 and B5) depicted a faster release of theophylline, with the drug releasing relatively quickly. This suggests that while the baobab polysaccharide can be effective for controlled release in acidic environments, it might not be suitable for targeting drug release in the lower small intestine or colon. These findings support the feasibility of a baobab-derived, renewable polysaccharide as an excipient aligned with our initial motivation to use green materials in pharmaceutical applications. Bench-scale extraction delivered approximately 20% yield, and the material formed mechanically robust, compressible tablets and provided sustained release in acidic medium with faster release in basic medium. This demonstrates the suitability of the formulations across conditions relevant to oral delivery. Moreover, these regionally sourced biopolymers could help diversify excipient supply chains where access to conventional materials is limited. Future work should address process standardisation, batch-to-batch variability, and safety/regulatory evaluation to translate this potential into practice.

## Conflicts of interest

The authors declare that they have no known competing financial interests or personal relationships that could have appeared to influence the work reported in this paper.

## Data availability

The authors confirm that the data supporting the findings of this study are available within the article.

## Acknowledgements

The authors are grateful to the University of Huddersfield for support.



## References

- 1 C. E. Beneke, A. M. Viljoen and J. H. Hamman, *Molecules*, 2009, **14**, 2602–2620.
- 2 D. A. Bhaskar, K. J. Uttam, A. Mahendrasingh, C. M. Jayram and S. R. Bhanudas, *J. Adv. Pharm. Educ. Res.*, 2013, **3**, 387–402.
- 3 M. Naghshineh, K. Olsen and C. A. Georgiou, *Food Chem.*, 2013, **136**, 472–478.
- 4 M. Wongkaew, B. Tinpovong, K. Sringarm, N. Leksawasdi, K. Jantanasakulwong, P. Rachtanapun and S. R. Sommano, *Foods*, 2021, **10**, 627.
- 5 P. M. Nadar, M. A. Merrill, K. Austin, S. M. Strakowski and J. M. Halpern, *Transl. Psychiatry*, 2022, **12**, 372.
- 6 M. J. Abdelhak, *J. Adv. Bio-Pharm. Pharmacovigil.*, 2019, **1**, 15–25.
- 7 E. I. Nep, N. Kaur, S. Shaboun, A. O. Adebisi, A. M. Smith, B. R. Conway and K. Asare-Addo, *Colloids Surf., B*, 2020, **188**, 110809.
- 8 K. Alba, M. Dimopoulou and V. Kontogiorgos, *LWT-Food Sci. Technol.*, 2021, **144**, 111235.
- 9 L. I. Atanase, *Polymers*, 2021, **13**, 477.
- 10 K. Alba, P. T. Nguyen and V. Kontogiorgos, *Food Hydrocolloids*, 2021, **118**, 106749.
- 11 X. N. Li, J. Sun, H. Shi, L. L. Yu, C. D. Ridge, E. P. Mazzola and P. Chen, *Food Res. Int.*, 2017, **99**, 755–761.
- 12 H. Bougatef, F. Tandia, A. Sila, A. Haddar and A. Bougatef, *S. Afr. J. Bot.*, 2023, **157**, 387–397.
- 13 K. Alba, V. Offiah, A. P. Laws, K. O. Falade and V. Kontogiorgos, *Food Hydrocolloids*, 2020, **106**, 105874.
- 14 F. M. Kpodo, J. K. Agbenorhevi, K. Alba, A. M. Smith, G. A. Morris and V. Kontogiorgos, *Int. J. Biol. Macromol.*, 2019, **122**, 866–872.
- 15 O. A. Patova, A. Luanda, N. M. Paderin, S. V. Popov, J. J. Makangara, S. P. Kuznetsov and E. N. Kalmykova, *Carbohydr. Polym.*, 2021, **262**, 117946.
- 16 C. D. May, *Carbohydr. Polym.*, 1990, **12**, 79–99.
- 17 J. Fan, K. Wang, M. Liu and Z. He, *Carbohydr. Polym.*, 2008, **73**, 241–247.
- 18 J. Liu, S. Willför and C. Xu, *Bioact. Carbohydr. Diet. Fibre*, 2015, **5**, 31–61.
- 19 R. Rojas, J. C. Contreras-Esquivel, M. T. Orozco-Esquivel, C. Muñoz, J. A. Aguirre-Joya and C. N. Aguilar, *Waste Biomass Valorization*, 2015, **6**, 1095–1102.
- 20 M. Dimopoulou, K. Alba, G. Campbell and V. Kontogiorgos, *J. Sci. Food Agric.*, 2019, **99**, 6191–6198.
- 21 M. Dimopoulou, K. Alba, I. M. Sims and V. Kontogiorgos, *Carbohydr. Polym.*, 2021, **273**, 118540.
- 22 E. I. Nep, K. Asare-Addo, M. U. Ghori, B. R. Conway and A. M. Smith, *Int. J. Pharm.*, 2015, **496**, 689–698.
- 23 H. Al-Hamidi, A. A. Edwards, D. Douroumis, K. Asare-Addo, A. M. Nayebe, S. Reyhani-Rad and A. Nokhodchi, *Colloids Surf., B*, 2013, **103**, 189–199.
- 24 M. M. Talukdar and R. Kinget, *Int. J. Pharm.*, 1995, **120**, 63–72.
- 25 K. Asare-Addo, M. Levina, A. R. Rajabi-Siahboomi and A. Nokhodchi, *Colloids Surf., B*, 2010, **81**, 452–460.
- 26 S. Dash, P. N. Murthy, L. Nath and P. Chowdhury, *Acta Pol. Pharm.*, 2010, **67**, 217–223.
- 27 P. Paarakh, P. Jose, C. Setty and P. Christoper, *Release Kinetics - Concepts and Applications*, 2018.
- 28 J. Siepmann and N. A. Peppas, *Adv. Drug Delivery Rev.*, 2001, **48**, 139–157.
- 29 J. Siepmann and F. Siepmann, *Int. J. Pharm.*, 2013, **453**, 12–24.
- 30 E. I. Nep, M. H. Mahdi, A. O. Adebisi, C. Dawson, K. Walton, P. J. Bills and K. Asare-Addo, *Int. J. Pharm.*, 2017, **532**, 352–364.
- 31 M. Dimopoulou, V. Offiah, K. Falade, A. M. Smith, V. Kontogiorgos and A. Angelis-Dimakis, *Sustainability*, 2021, **13**, 9915.
- 32 A. Charlesby, *J. Polym. Sci.*, 1953, **11**, 521–529.
- 33 N. S. Murthy and F. Reidinger, *X-ray Analysis. A Guide to Materials*, 1996.
- 34 B. A. Stone, B. Svensson, M. E. Collins and R. A. Rastall, *Glycoscience*, 2008, 2325.
- 35 Y. Peng and S. Wu, *J. Anal. Appl. Pyrolysis*, 2010, **88**, 134–139.
- 36 M. S. Iqbal, S. Massey, J. Akbar, C. M. Ashraf and R. Masih, *Food Chem.*, 2013, **140**, 178–182.
- 37 M. El-Sakhawy and M. L. Hassan, *Carbohydr. Polym.*, 2007, **67**, 1–10.
- 38 N. Saigal, S. Baboota, A. Ahuja and J. Ali, *J. Young Pharm.*, 2009, **1**, 6.
- 39 K. Asare-Addo, B. R. Conway, M. J. Hajamohaideen, W. Kaialy, A. Nokhodchi and H. Larhrib, *Colloids Surf., B*, 2013, **111**, 24–29.
- 40 K. M. Keogh, F. J. O'Brien and N. J. Dunne, *Front. Mater.*, 2021, **8**, 752813.
- 41 Y. Qiu and K. Park, *Polymers*, 2017, **9**, 137.

